JMSAE Journal of Materials Science and Applied Energy

Journal home page: jmsae.snru.ac.th

Heating Performance of Indium Tin Oxide Transparent Heating Element

Wanichaya Mekprasart, Phongpisut Nawongsri, Wisanu Pecharapa*

College of Nanotechnology, King Mongkut's Institute of Technology Ladkrabang, Bangkok, 10520 Thailand

*Corresponding Author: wisanu.pe@kmitl.ac.th

Received 27 January 2021; **Revised** 5 February 2021; **Accepted** 4 June 2021; **Available online:** 1 September 2021

Abstract

Indium tin oxide (ITO) is one of transparent conducting oxide material which is widely used in electronic industries. The objective of this research is to study thermal performance of ITO heating element stripe fabricated with various sizes and widths. The pattern was designated and fabricated by the acid etching process using aqua-regia whose ratio of hydrochloric acid to nitric acid is fixed at 3:1. Three different widths of 4 mm, 5 mm and 6 mm were designated and patterned. In heating performance testing, various voltages were directly supplied to the elements leading to the elevating temperature as a function of time. It was found that the optimized pattern with width of 6 mm performed excellent electrical heating temperature up to 110 °C at bias voltage of 15 V. The rising and falling time constant of ITO heating elements at 6 mm were also determined as 59.70 s and 68.61 s.

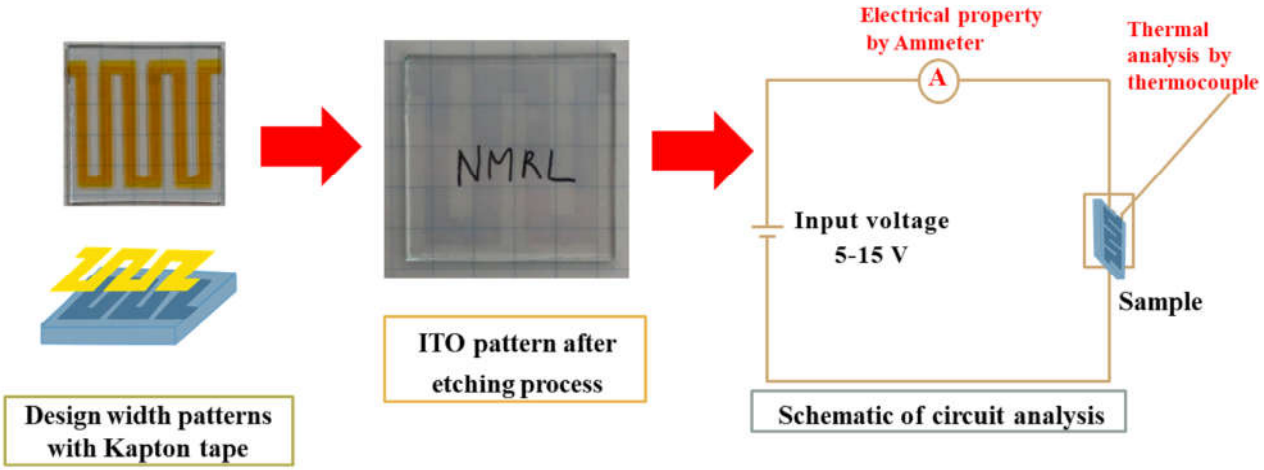

Keywords: Electrical property; Heating element; Indium tin oxide; Thermal performance

Introduction

Transparent conducting oxides (TCOs) have been a greatly attractive semiconductor material in the recent decades due to its good electrical conductivity with 80% optical transmittance of incident light. TCOs are binary or ternary metal oxide compounds which are composed of one or two metallic elements. Low resistivity in TCOs material could be as low as 10^{-4} Ω cm, with extinction coefficient (k) in optical visible range (VIS) lower than 0.0001, owing to wide optical band gap ($E_g > 3$ eV) [1]. These remarkable properties of conductivity and transparency in TCOs can be originated by the addition of dopant in intrinsic stoichiometric oxide. Metal oxide materials as ZnO, SnO_2, In_2O_3 and their alloys were also categorized as highly efficient TCOs [2]. Their prominent properties in electrical conductivity and optical transmission could be improved by doping with some metal such as Al-doped ZnO (AZO), Sn-doped In_2O_3 (ITO), and antimony or fluorine doped SnO_2 (ATO or FTO) with thin film technology [3]. Among the most utilized TCOs materials, ITO is used extensively in wide range because of its rather low electrical resistivity with low an absorption coefficient (α) in the near-UV and VIS range and with an optical band gap between 3.50 and 4.30 eV [4]. Therefore, ITO material has been widely applied in electronic industries, for example, touch screen panel, OLEDs, transparent electrodes and photovoltaic devices [5 – 9]. Meanwhile, ITO is one of the most promising for heat-generating material in from of transparent heater device. The fabrication of ITO nanoparticles (NPs) on flexible plastic substrates could be utilized as fabricated heater at relatively low temperature and cost [10]. The modification of ITO nanoparticles and silver nanowires (Ag NWs) in composite structure on photo-polymeric film was proposed for flexible transparent heater with ultrahigh thermal efficiency and fast thermal response speed [11]. While, ITO thin film was applied to interdigit structured electrodes (IDE) and a micro heater with high transmittance and low resistivity properties for the cooperation with transparent gas sensor [12]. A transparent thermal source in a microchannel chip for polymerase chain reactions was developed by a flat ITO heater [13]. However, shape designs of the heating path on ITO film have been importantly considered that could be related to facile control of the thermal state on the heaters [14]. Therefore, width pattern on ITO film is a key role on thermal property for energy transfer to other devices. Meanwhile, the difference of ITO width and size is corresponded to its resistance and current density inside the pattern as described by Joule heating effect [15]. In this work, three different widths in millimeter scale were designated and patterned on ITO surface by chemical etching process to study its electrical and thermal properties. Moreover, thermal time constant was calculated to identify its responsibility after electrical activation and cool down stage.

Materials and Methods

Commercial ITO glass with resistivity 15 Ω sq^{-1} was cut with area 2.50 × 2.50 cm^2. Each cleaning step for ITO glasses was soaked at 10 min by ultrasonic assisted alcohol process with DI water, acetone, methanol and isopropanol, respectively. Dry process was required for ITO sample at 100 ºC with short period. The width of element strips on ITO glass was designed at 4 mm, 5 mm and 6 mm and fabricated in interdigit pattern with kapton tape on ITO film as presented in Fig. 1. After that, the samples were etched in aqua regia solution with the ratio of $HCl:HNO_3$ at 3:1 for 30 – 60 s and rinsed with DI water and ethanol to remove acid solution on film surface.

Then, kapton tape was removed after heat treatment. Finally, ITO pattern films with different widths were successfully obtained by simple patterning and etching process.

Thermal and electrical properties of etching ITO samples with different widths were monitored by series circuit as depicted in Fig. 2. DC power supply as electrical source was used as voltage generator in range of 5 – 15 V in circuit analysis. Rising temperature and flow current on design samples were monitored every 10 s by thermocouple and digital multimeter. After that, voltage generator was dropped to 0 V and instant temperature was recorded every 10 s. Electronic parameters of resistance and resistivity of ITO films with different widths were determined and followed by Ohm's law and Pouillet's law [16]. Meanwhile, thermal time constant of rising and falling temperature on the sample was determined by naturally exponential decay equation as shown in equation (1);

$$T_f = (T_f - T_i)(1 - e^{(-t/\tau)}) + T_i \quad (1)$$

where T_t is temperature of the patterned film element measured at specific time t, T_i is the initial temperature, T_f is final temperature, t is the elapsed time and τ is characteristic time constant for either raising time constant (heating) or falling time constant (cooling). T_i, T_f and τ can be determined by best fitting as rising time constant was evaluated at 63.20% of ΔT while falling time constant was evaluated at 36.80% of ΔT

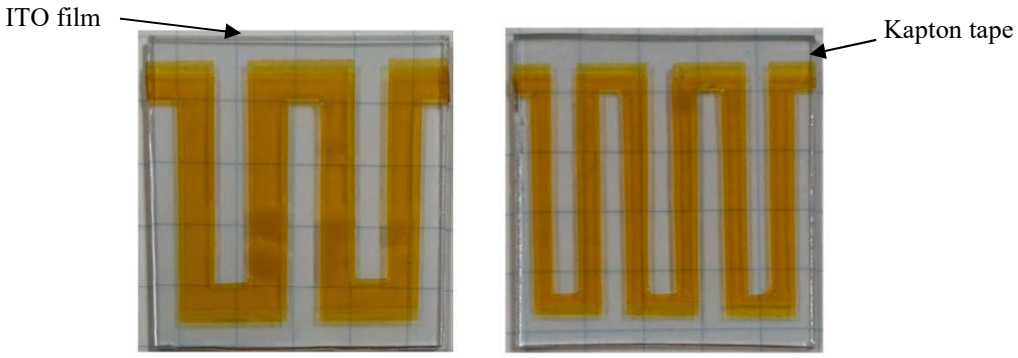

Fig. 1 Examples of ITO width patterning film with kapton tape design (yellow pattern on ITO film).

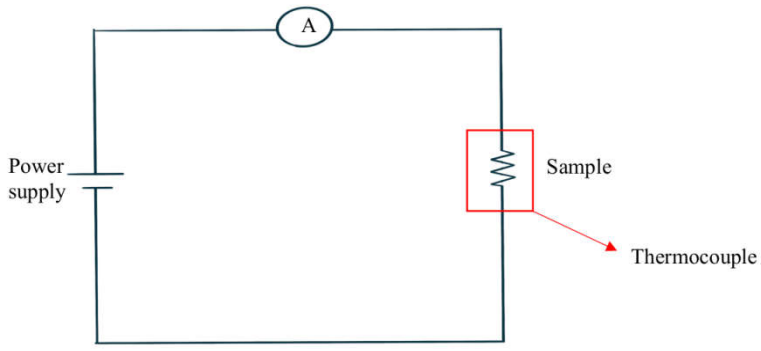

Fig. 2 Series circuit of ITO samples with different width patterns for thermal and electrical analysis.

Results and Discussion

The steady-state temperatures measured for ITO films with different width patterns as a function of time for various bias voltages in range of 5 – 15 V are depicted in Fig. 3. For the beginning state at 0 – 50 s, the temperature on ITO film drastically increased from room temperature due to no input inside the film relating to high temperature rate. Meanwhile, the temperature on ITO plate slightly increased in range of 50 – 150 s. After time operation at 150 s, temperature tended to reach the steady point owing to current equilibrium state and the system reached the thermal equilibrium. It can be concluded that the steady-state temperature is reached within 100 s for all bias voltages.

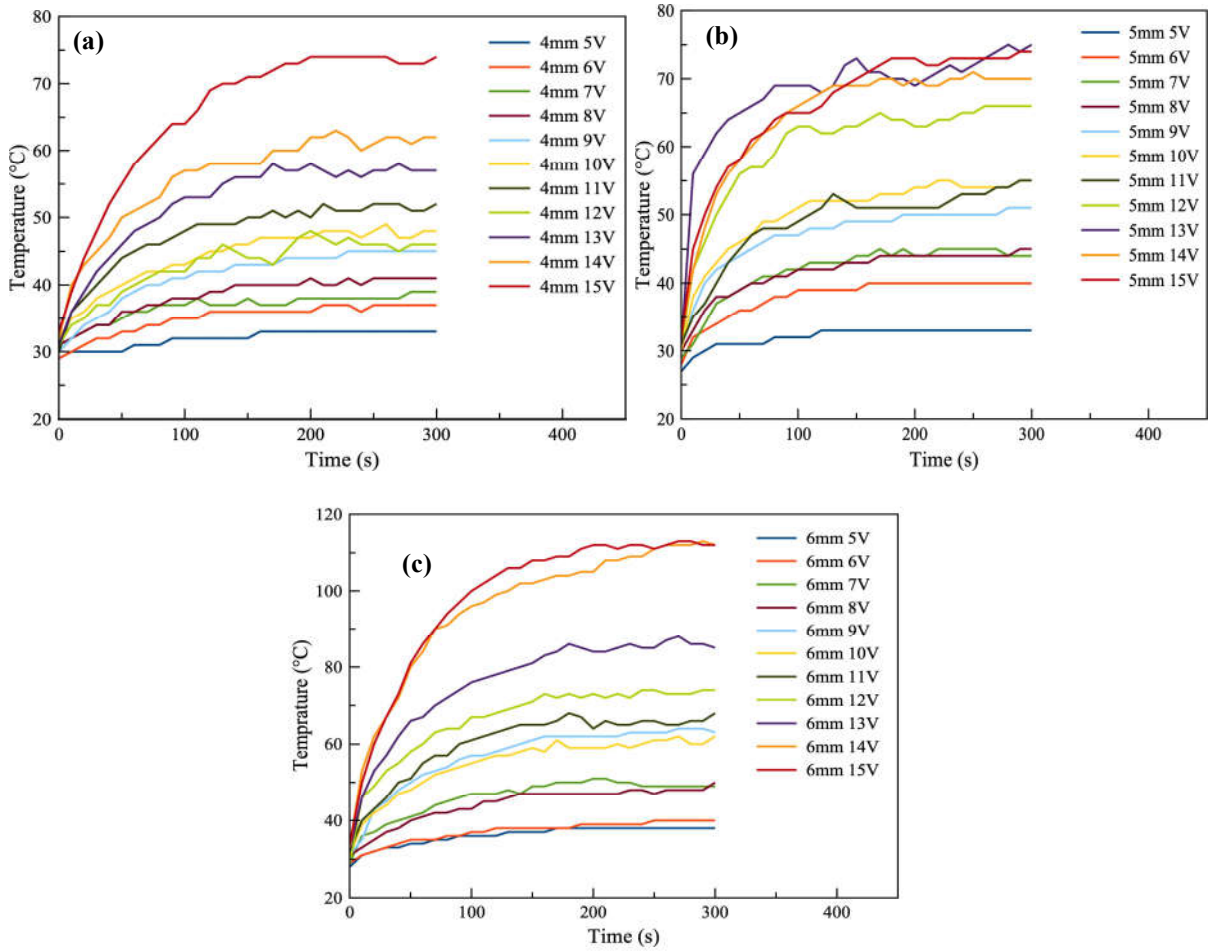

Fig. 3 Steady-state temperature measured as a function of time on ITO films with different widths (a) 4 mm, (b) 5 mm and (c) 6 mm biased with various voltages in range of 5 – 15V.

Steady-state temperature of the samples with pattern width of 4 and 5 mm reaches to 75 ºC with maximum input voltage of 15 V. Meanwhile, the highest temperature on ITO film at width pattern of 6 mm occurred at 110 ºC due to large surface area on width size relating to high thermal energy consumption. This heating mechanism can be explained by joule heating effect [15] confirming by increasing temperature with increasing current provided by higher bias voltage. Therefore, if the width pattern increases to be greater than 6 mm, its resistance will consequently decrease and greater current will flow through the pattern resulting in the greater heat dissipated in the pattern and also the increase in temperature. Moreover, each sample applied maximum voltage

at 15 V was related to the highest current inside the width. Hence, lower resistance was obtained at the widest width of 6 mm corresponding to the highest current on ITO film according to linear equation of Ohm's law (equation (2)).

The steady-state current measurement in the circuit was monitored on ITO patterned films with different widths under various input voltages at 5 – 15 V as presented in Fig. 4. Flow current is in steady-state for all of the bias voltages after some certain time. Steady-state current on width pattern at 4, 5 and 6 mm is obtained at 88.80, 132.00 and 147.70 mA at maximum voltage of 15 V. The highest current on ITO film was found in the sample with width of 6 mm. However, the increase of flow current was significantly occurred during 0 – 100 s at higher input bias (more than 10 V). This phenomenon can be described by the relation between resistance and temperature. High resistance of the load was occurred at low temperature resulting to unsteady current during initial operating time in 0 – 100 s. Meanwhile, the current was constant in range of 100 – 300 s because of stable temperature on ITO surface.

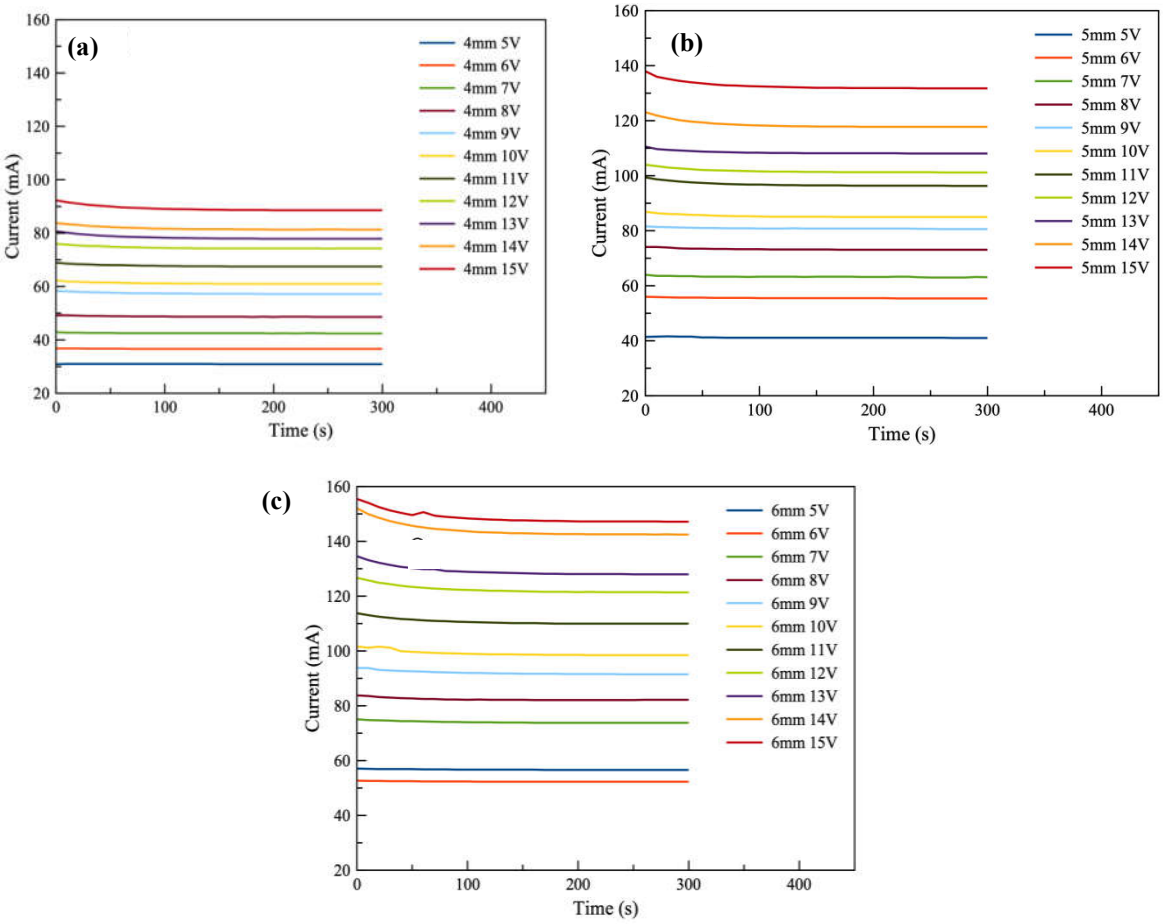

Fig. 4 Steady-state current measured as a function of time on ITO films with different widths (a) 4 mm, (b) 5 mm and (c) 6 mm biased with various voltages in range of 5 – 15V.

After biased voltage was turned off, temperature on ITO surface at all width conditions exponentially decreased as shown in Fig. 5, as designated as cooling stage. Final temperature on ITO surface can be reached to room temperature after the biased voltage was turned off for 300 s. The resistance of ITO patterned element with different widths as shown in Table 1 was determined by the relation of resistance and resistivity followed by equation (2) – (4);

Ohm's law; $$V = IR \tag{2}$$

and Pouillet's law; $$R = \frac{\rho \ell}{A} = \frac{\rho \ell}{Wd} \tag{3}$$

Hence; $$\rho = \frac{RWd}{\ell} \tag{4}$$

where, V is input voltage (V), I is flow current (A), R is resistance (Ω), ρ is the resistivity (Ωmm), W is ITO pattern width (mm), d is film thickness (mm) and ℓ is ITO path length (mm). Following equation (2), the decrease in resistance was distinguishably obtained with increasing ITO width due to high flow current in the circuit at high bias voltage. From equation (3) and (4), electrical resistivity of ITO with different widths are in the range of $1.20 \times 10^{-3} – 1.80 \times 10^{-3}$ Ω mm. The slight change in the resistivity value could be due to bless path length from width design that shown in ITO width pattern of 6 mm. However, the changing of electrical resistivity may be occurred by the physical properties of material such as crystallinity, charge carrier and carrier concentrations. Therefore, a bit of resistivity changing was influenced by the amount of charge carrier and carrier concentrations in different widths [17].

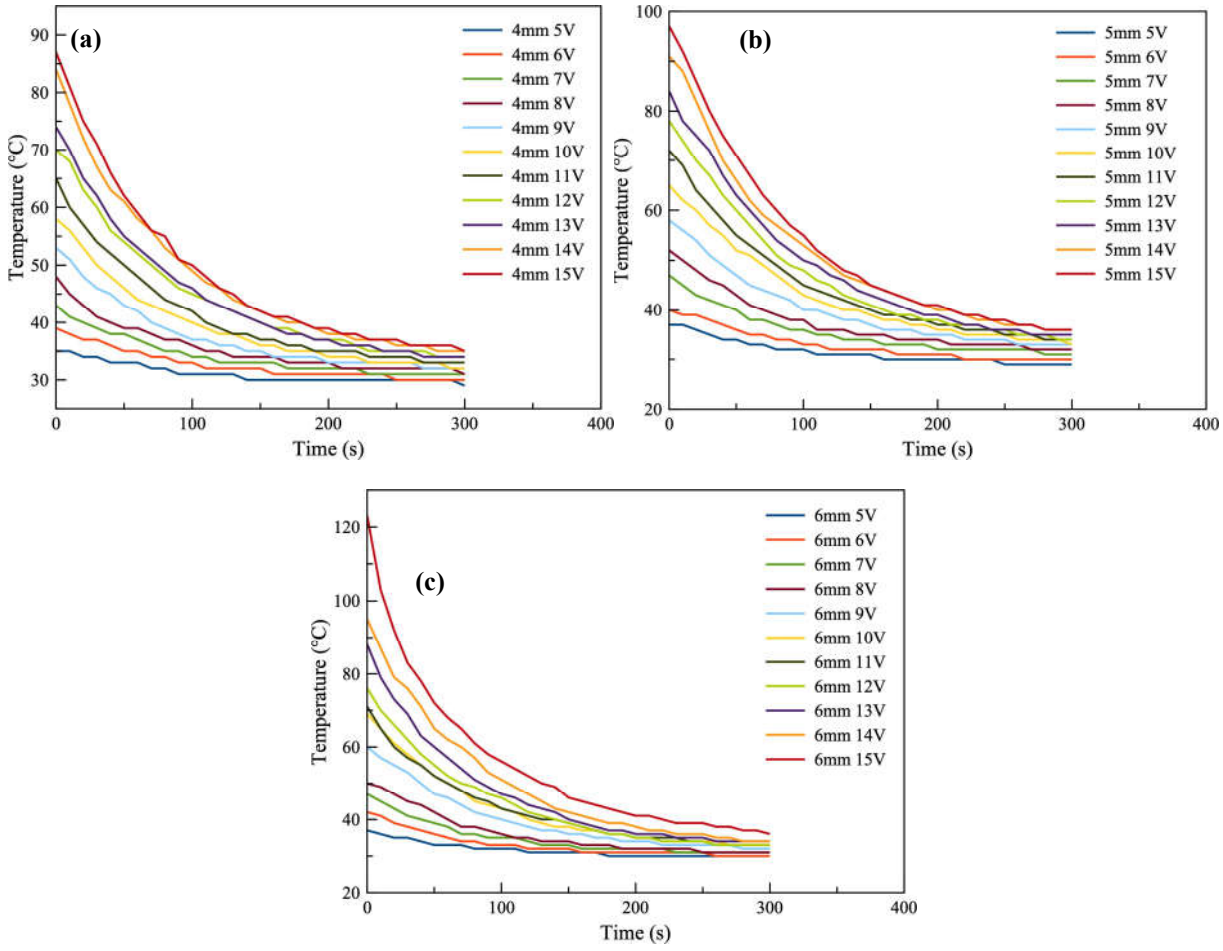

Fig. 5 Decreasing temperature on ITO film with different widths at (a) 4 mm, (b) 5 mm and (c) 6 mm without input voltage.

High efficiency in thermal and electrical properties was optimized in the sample with 6 mm ITO width at maximum voltage of 15 V. Therefore, this condition was chosen to further verify cycle efficiency. During 0 – 300 s, ITO sample was operated under input voltage at 15V. Steady temperature and current was still similar result as described in Fig. 1 and 2. After the biased voltage was decreased to 0 V in range of 300 – 600 s, the element was in cooling stage as shown in Fig. 3. No input voltage was affected on the absence of current flowing inside the width relating to decreasing temperature to room temperature. Then, ITO film was in turn-on state again and it exhibited the same pattern with steady temperature and current as first cycle. These graphs indicated good repeatability in the current and temperature of this fabricated heating element.

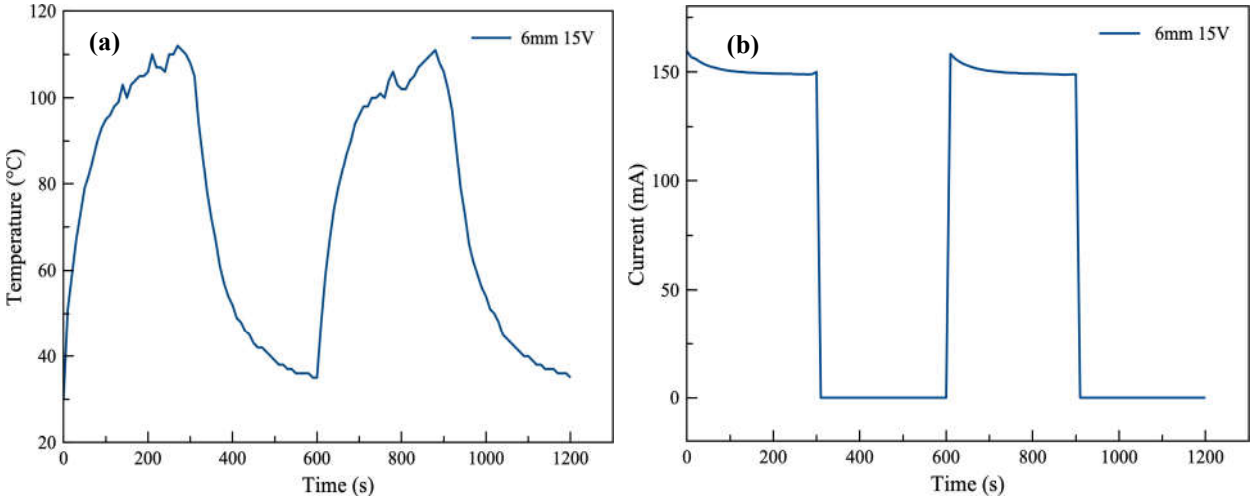

Fig. 6 The cycle of (a) temperature and (b) current on ITO sample at width 6 mm under 15 V.

Table 1 Electronic parameters of ITO thin films with different widths.

ITO width; W (mm)	Length; ℓ (mm)	Thickness; d (nm)	Resistance; R (Ω)	Resistivity; ρ (Ω mm)
4	58.50	109	164.30	1.22×10^{-3}
5	53.00	109	114.85	1.81×10^{-3}
6	48.00	109	99.39	1.35×10^{-3}

Table 2 Thermal time constant of rising/falling state of ITO films with different widths.

ITO width; W (mm)	Rising Time Constant; Γ_{rise}(s)	Falling Time Constant; Γ_{fall}(s)
4	42.38	74.81
5	61.36	78.75
6	59.70	68.61

Thermal time constant in rising state is defined as the time for high temperature on heating element without other loads in the circuit that changed to 63.20% of the difference between the initial and final temperature during the surrounding temperature [1]. Meanwhile, falling time

constant is determined by equation (1) at 36.80% of the difference between their highest and room temperatures. Its value is much larger than that of rising time constant because heat outflows from ITO heating element is naturally released by thermal convection and radiation after bias voltage is turned off. The values of rising time constant and falling time constant in each ITO heating element were calculated and shown in Table 2. Minimum rising time constant was occurred at 42.38 s from ITO width of 4 mm due to its narrow width relating to facile heat transfer inside path length. Meanwhile, the element with wider width showed high rising time constant of 60 s. In case of cooling state, the element with the width of 6 mm exhibited high responsibility of heat transfer from surface sample to surrounding environment due to its larger surface area. Therefore, the heating element with the width of 6 mm shows the optimized condition for heat element that rising to the highest temperature and current on ITO surface. Meanwhile, it can be cooled down to ambient temperature with less time.

Conclusion

Electrical and thermal properties of ITO thin film are depended on width patterns. The improvement of electrical conductivity and heating rate was obviously obtained by large ITO width size at 6 mm. By this optimized condition, less resistance and high surface area leads to the increase in flow current and thermal energy transfer inside ITO pattern. Meanwhile, the ITO heating element with pattern width of 6 mm was also good candidate as heating element due to proper condition of thermal time constant in heating and falling state. From this work, suitable temperature range of ITO heating element should be chosen by the variation of width patterns on ITO thin film depending on the applications.

Acknowledgement

This work has partially been supported by College of Nanotechnology, King Mongkut's Institute of Technology Ladkrabang (KMITL) for supporting laboratory facilities and material characterization.

References

[1] G. Brunin, F. Ricci, V.A. Ha, G.M. Rignanese, G. Hautier, Transparent conducting materials discovery using high-throughput computing, Npj Comput. Mater. 5 (2019) 63.

[2] T. Minami, Transparent conducting oxide semiconductors for transparent electrodes, Semicon. Sci. Technol. 20(4) (2005) S35 – S44.

[3] A. Klein, C. Körber, A. Wachau, F. Säuberlich, Y. Gassenbauer, S.P. Harvey, D.E. Proffit, T.O. Mason, Transparent conducting oxides for photovoltaics: manipulation of fermi level, work function and energy band alignment, Materials. 3(11) (2010) 4892 – 4914.

[4] J.W. Wang, F.F. Luo, G.X. Ouyang, Y. Shi, Magnetic, optical and electrical properties of ITO thin films implanted by cobalt ions, Nucl. Instrum. Methods Phys. Res. B. 450 (2019) 234 – 238.

[5] C.C. Wu, Ultra-high transparent sandwich structure with a silicon dioxide passivation layer prepared on a colorless polyimide substrate for a flexible capacitive touch screen panel, Sol. Energy Mater. Sol. Cells. 207 (2020) 110350.

[6] Z. Li, X. Li, X. Lin, H. Wang, Y. Fu, B. Zhang, J. Wu, Z. Xie, Highly efficient organic light-emitting diodes employing the periodic microstructured ITO substrate fabricated by holographic lithography, Org. Electron. 75 (2019) 105438.

[7] S.Y. Bao, X. Deng, F. Mao, N. Zhong, F.Y. Yue, L. Sun, P.H. Xiang, C.G. Duan, Ultra-flat ITO films on mica for high temperature transparent flexible electrodes, Ceram. Int. 46(2) (2020) 2268 – 2272.

[8] D.A. Álvarez, L.F. Llin, A. Mellor, D.J. Paul, N.J. Daukes, ITO and AZO films for low emissivity coatings in hybrid photovoltaicthermal applications, Sol. Energy. 155 (2017) 82 – 92.

[9] K. Lim, S. Jung, J.K. Kim, J.W. Kang, J.H. Kim, S.H. Choa, D.G. Kim, Flexible PEDOT:PSS/ITO hybrid transparent conducting electrode for organic photovoltaics, Sol. Energy Mater. Sol. Cells 115 (2013) 71–78.

[10] K. Im, K. Cho, K. Kwak, J. Kim, S. Kim, Flexible transparent heaters with heating films made of indium tin oxide nanoparticles, J. Nanosci. Nanotechnol. 13(5) (2013) 3519 – 3521.

[11] C. Kim, M.J. Lee, S.J. Hong, Y.S. Kim, J.Y. Lee, A flexible transparent heater with ultrahigh thermal efficiency and fast thermal response speed based on a simple solution-processed indium tin oxide nanoparticles-silver nanowires composite structure on photo-polymeric film, Compos. Sci. Technol. 157 (2018) 107 – 118.

[12] T.J. Hsueh, C.H. Peng, W.S. Chen, A transparent ZnO nanowire MEMS gas sensor prepared by an ITO microheater, Sens. Actuators B Chem. 304 (2020) 127319.

[13] K. Sun, A. Yamaguchi, Y. Ishida, S. Matsuo, H. Misawa, A heater-integrated transparent microchannel chip for continuous-flow PCR, Sens. Actuators B Chem. 84 (2002) 283 – 289.

[14] R. Pawlak, M. Lebioda, Electrical and thermal properties of heater-sensor microsystems patterned in TCO films for wide-range temperature applications from 15 K to 350 K, Sens. 18 (2018) 1831.

[15] N.J. Petersen, R.P.H. Nikolajsen, K.B. Mogensen, J.P. Kutter, Effect of Joule heating on efficiency and performance for microchip-based and capillary-based electrophoretic separation systems: A closer look, Electrophoresis. 25 (2004) 253 – 269.

[16] H. Hosono, K. Ueda, Transparent Conductive Oxides. Springer Cham, New York, 2017.

[17] A.H. Ali, Z. Hassan, A. Shuhaimic, Enhancement of optical transmittance and electrical resistivity of post-annealed ITO thin films RF sputtered on Si, Appl. Surf. Sci. 443 (2018) 544 – 547.